buildings

MDPI

Article

Hourly Calculation Method of Air Source Heat Pump Behavior

Ludovico Danza [1,*], Lorenzo Belussi [1], Italo Meroni [1], Michele Mililli [2] and Francesco Salamone [1]

[1] Construction Technologies Institute of National Research Council of Italy, Via Lombardia 49, San Giuliano Milanese, Milano 20098, Italy; belussi@itc.cnr.it (L.B.); meroni@itc.cnr.it (I.M.); salamone@itc.cnr.it (F.S.)

[2] D'Appolonia S.p.A., Via A. Liri 27, Genova 16145, Italy; michele.mililli@dapollonia.it

* Correspondence: danza@itc.cnr.it; Tel.: +39-02-9806-424

Academic Editor: Christopher Underwood

Received: 1 February 2016; Accepted: 1 April 2016; Published: 5 April 2016

Abstract: The paper describes an hourly simplified model for the evaluation of the energy performance of heat pumps in cooling mode maintaining a high accuracy and low computational cost. This approach differs from the methods used for the assessment of the overall energy consumption of the building, normally placed in the so-called white or black box models, where the transient conduction equation is deterministically and stochastically solved, respectively. The present method wants to be the expression of the grey box model, taking place between the previous approaches. The building envelope is defined using a building thermal model realized with a 3 Resistance 1 Capacitance (3R1C) thermal network based on the solution of the lumped capacitance method. The simplified model evaluates the energy efficiency ratio (EER) of a heat pump through the determination of the hourly second law efficiency of a reversed Carnot cycle. The results of the simplified method were finally compared with those provided by EnergyPlus, a dynamic building energy simulation program, and those collected from an outdoor test cell in real working conditions. The results are presented in temperatures and energy consumptions profiles and are validated using the Bland-Altman test.

Keywords: hourly simplified model; RC model; heat pump; EER; reversed Carnot cycle

1. Introduction

The increasing demand for building services has persuaded the EU to take decisive measures for energy efficiency. The building sector represents 40% of the European Union's energy consumption [1]. Through the so called Europe 2020 Strategy, the European Commission set the ambitious goal to improve the energy efficiency of each state by increasing the energy production by renewable sources aimed at the reduction of greenhouse gases, confirmed by the recent Europe 2030 Strategy. In this context, the improvement of the performance of buildings plays a key role, both by reducing the energy losses and by using high-performance systems and renewable energy sources [2]. The new paradigm requires a new concept of building energy simulation (BES) software by integrating the real and the predicted performance [3–6], by considering the real working conditions of buildings [7–10] and the real external data [11].

According to the EN ISO 15603 [12], the methods used for the assessment of the overall energy consumption of the building can be divided into two main categories, measured and calculated. The former is based on the monitoring of energy consumption and other physical parameters of buildings during the operational phase. The latter is based on more or less complex algorithms of the heat balance equations of buildings as a function of the level of detail of the analysis. This approach can be itself divided into two sub-categories: steady-state or quasi-steady-state methods, calculating

the heat balance over a sufficient time period, during which the dynamic effects are taken into account by an empirically gain/loss utilization factor; and dynamic methods, calculating the heat balance with short time steps taking into account the heat stored and released from the mass of the building. The performance of these methods has been assessed [13–16] with different degree orders as a function of the building's characteristics [17].

The hourly calculation methods based on the lumped capacitance-resistance (RC) network model take place between these approaches. Several studies demonstrate how the results of the RC models are close to the real energy behavior of buildings [18–21]. The RC models are applied to the building envelope, with different degree orders, as a function of the number of the considered capacitances [22]. Equivalent RC schemes are broadly used to represent thermal systems. This method of representation arises from the lumped capacitance solution of transient heat transfer equations, a well-known consequence of the thermal-electric analogy. This is clearly not the case of the building envelope, where sparse temperature distributions come along with heat sinks (thermal bridges, air gaps, *etc.*) and gains (solar radiation, *etc.*). Although this approach cannot represent a fine temperature distribution, it is a good candidate to represent the overall thermal behavior of a building. The lumped parameter models take place in the so-called grey box approach, *i.e.*, a tool for identifying system characteristics from physical and measured data, different from the white-box and black-box approaches, where the physical behavior is completely known and stochastically estimated, respectively [23]. The evaluation of the plant performance can be carried out following the different approaches [24]. Next to the well-established white- and black-box approaches in recent years, the scientific community has focused attention on the next level by incorporating the lumped parameter model with systems and controls [25], with a focus on the heat pump system [26,27], also combined with other approaches [28]. In the present article, the lumped RC model is combined with a simplified hourly method for the calculation of the thermal and energy performance of a heat pump. The envelope was represented by a 3 Resistance 1 Capacitance (3R1C) network in which the components are connected each other through the internal air temperature node. The overall behavior of the building envelope is completed described by the differential equations of transient heat conduction. The heat pump behavior is completely described by the equations governing the thermodynamic cycle, according to the white box approaches. The basis of the developed model is the second law efficiency through the reversed Carnot cycle, which has been adapted to an hourly method.

The calculation of the hourly consumption of the heat pump is based on the evaluation of the coefficient of performance in winter (COP) and the energy efficiency ratio in summer (EER), which is calculated through the values of the hourly average temperature of the refrigerant fluid in the condenser and in the evaporator of the heat pump. These temperatures are calculated using some complex relations starting from the energy needs of an envelope [29]. The so-defined calculation method is tested in real working conditions through a seasonal experimentation in real test cell equipped with a heat pump with pre-defined use profiles and control setup. The test was conducted starting from the co-heating test methodology [30], properly applied to evaluate the performance of the air condition system. Finally, to evaluate the suitability of the model, a comparison with the results obtain with EnergyPlus [31] are presented, which is one of the widespread building energy simulation (BES) programs, an expression of the black-box approach.

2. Simulation and Experiment

2.1. Heat Pumps

Heat pumps have become increasingly widespread in European countries [32] thanks to several factors (policies, infrastructural facilities, research and development) [33]. The recent international directives regarding the energy performance of buildings have greatly contributed to the establishment of such devices.

In general, a heat pump follows the principle of the reversed Carnot cycle, consisting of two isotherms and two adiabatic transformations.

The difficulties that are encountered while practically performing the reversed Carnot cycle can be overcome by performing the ideal reverse steam compression cycle [34]. In this case, as shown on the plan entropy-temperature (ST) in Figure 1, the heat absorption continues until reaching the condition of dry saturated steam (point 2), so that subsequent isentropic compression occurs in the superheated steams zone (segment 1–2).

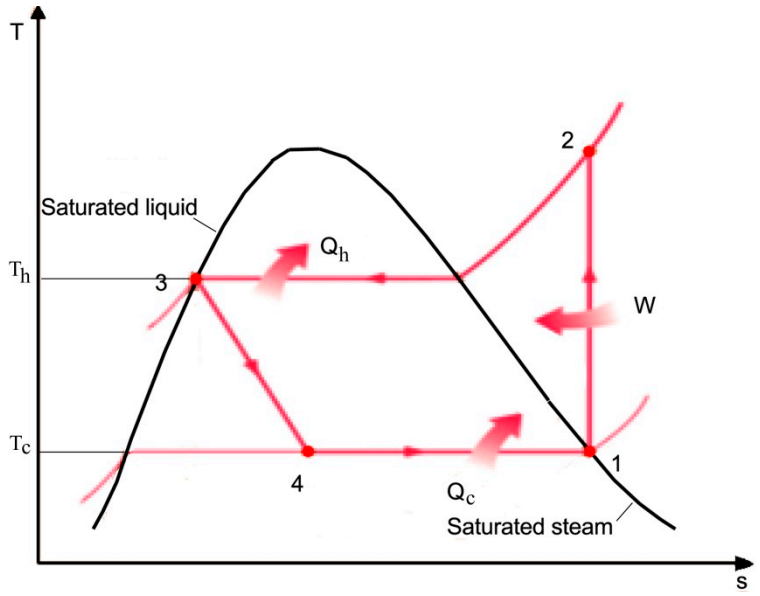

Figure 1. Refrigeration cycle represented on the entropy-temperature plan (s-T): 1–2 compressor; 2–3 condenser; 3–4 expansion valve; 4–1 evaporator.

After being compressed, the fluid is desuperheated and condensed to become a saturated liquid, passing in the condenser (segment 2–3) and releasing heat to the external environment. Following segment 3–4, the fluid is expanded through an expansion valve. Finally, entering the evaporator (segment 4–1), the fluid absorbs heat and is transformed again into saturated steam. In this regard, the compression refrigeration cycle is better suited for the purposes of a heat pump.

The performances of a heat pump are determined by considering the COP and the EER in the heating and the cooling seasons, respectively.

COP and EER are given by the relation between the useful effect (Q_h, in winter or Q_c, in summer) and the energy supplied (W), according to the following formulas:

$$COP = \frac{Q_h}{W} \quad (1)$$

$$EER = \frac{Q_c}{W} \quad (2)$$

In the ideal case, by adopting the reversed Carnot cycle, knowing that:

$$Q_h = Q_c + W \quad (3)$$

The ideal COP and EER are given by:

$$COP_{id} = \frac{T_h}{T_h - T_c} \quad (4)$$

$$EER_{id} = \frac{T_c}{T_h - T_c} \quad (5)$$

where:

T_c is the absolute temperature of the cold reservoir (K),

T_h is the absolute temperature of the hot reservoir (K).

With a few simple steps, a direct relation between COP_{id} and EER_{id} is obtained as follows:

$$COP_{id} = \frac{T_h}{T_h - T_c} = \frac{T_h - T_c + T_c}{T_h - T_c} = 1 + \frac{T_c}{T_h - T_c} = 1 + EER_{id} \quad (6)$$

2.2. Calculation Model

The work carried out aims at identifying a methodology for the hourly calculation of the performances of a heat pump and the associated consumption. The model is developed on the basis of the international standard EN 15316-4-2:2008 [35], where monthly weather data are sorted into discrete groups (bin method), adapted to an hourly calculation.

In particular, the following relation takes place:

$$EER = \eta_{II} \cdot EER_{id} \quad (7)$$

where η_{II} is the second law efficiency.

To determine the value of the second law efficiency, with the known temperature values of the heat sink and the cold source, respectively, it is necessary to perform a double interpolation starting from two known values of temperature for the heat sink, $T_{h,1}$ and $T_{h,2}$, and two known values of temperature for the cold source, $T_{c,1}$ and $T_{c,2}$, generally supplied by the manufacturer.

Hence, the following equation:

$$\eta_{II}(T_h/T_c) = \eta_{II}(T_{h,1}/T_{c,1}) + \frac{\eta_{II}(T_h/T_{c,2}) - \eta_{II}(T_h/T_{c,1})}{(T_{c,2} - T_{c,1})} \cdot (T_c - T_{c,1}) \quad (8)$$

where:

$$\eta_{II}(T_h/T_{c,1}) = \eta_{II}(T_{h,1}/T_{c,1}) + \frac{\eta_{II}(T_{h,2}/T_{c,1}) - \eta_{II}(T_{h,1}/T_{c,2})}{(T_{h,2} - T_{h,1})} \cdot (T_h - T_{h,1}) \quad (9)$$

$$\eta_{II}(T_h/T_{c,2}) = \eta_{II}(T_{h,1}/T_{c,2}) + \frac{\eta_{II}(T_{h,2}/T_{c,2}) - \eta_{II}(T_{h,1}/T_{c,2})}{(T_{h,2} - T_{h,1})} \cdot (T_h - T_{h,1}) \quad (10)$$

The temperatures T_h and T_c are calculated to perform the hourly calculation of the EER. The calculation of these temperatures requires knowing the thermodynamic properties of the refrigerant used by the heat pump, in this case R410A.

The procedure used to determine the temperatures T_h and T_c is rather complex and is based on a number of assumptions. However, the adoption of an iterative process makes it possible to reduce to acceptable levels the errors due to the initial approximations.

According to the manufacturer information, the superheating of the refrigerant is set at 7 K beyond the saturated steam curve (segment 1–1′ in Figure 2) in order to prevent the refrigerant from entering the compressor in the liquid state, because the real cycle is less predictable than the ideal cycle. In the case, instead, of the expansion process the design practice recommends to subcool a refrigerant by 5 K beyond the saturated liquid curve (segment 3–3′ in Figure 2) in order to improve the overall efficiency of the system.

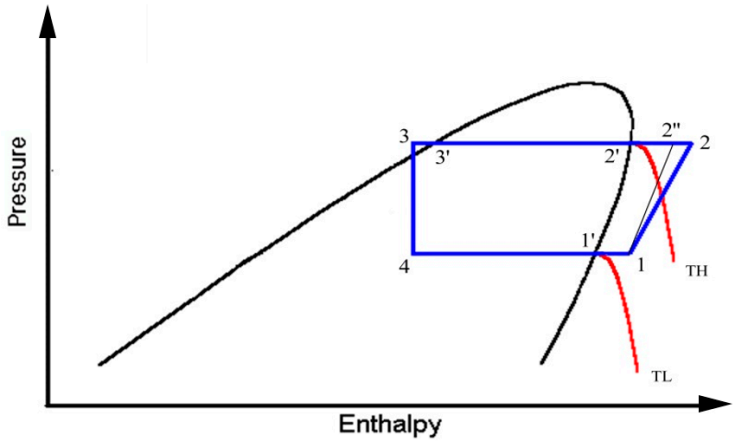

Figure 2. Refrigeration cycle represented on the enthalpy-pressure plan (p-H).

First, the temperature of the refrigerant at the saturation points is obtained by knowing the thermodynamic properties of the refrigerant along the curve formed by the points of the saturated liquid and steam, by intersecting it with the enthalpy of saturation or the corresponding pressure. At this time, the procedure of calculation has been implemented, referring to which general refrigeration cycle is taken on (Figure 2), which should be representative of the generic cycle of a refrigerating machine, illustrated in the enthalpy-pressure plan (p-H).

Contrary to the refrigerant cycle, it is necessary to proceed in reverse order starting from point 1 to determine the position of the real cycle in the diagram.

It is necessary to know the energy needs, *i.e.*, the quantity of heat to be removed from the environment, for each hour and for a set-point temperature.

$$\Delta h_{41} = \frac{Q_{H,nd}}{q} \tag{11}$$

where:

$Q_{H,nd}$ is the energy need of the building envelope,

q is the mass flow rate of the cooling fluid.

Once Δh_{41} is known, starting from the superheated steam at point 1 and at unknown pressure, the enthalpy at point 4 is determined.

Considering that the expansion process, which is based on the conservation of energy principle, takes place in an isenthalpic manner, disregarding the error given by the irreversibility of the process, the following equation is defined:

$$h_4 = h_3 \tag{12}$$

It is possible to graphically plot point 3 intersecting the isenthalpic passing through point 4 with an isobar whose segment 3–3′ is equal to 5 K, that corresponds to the difference between the subcooled liquid temperature (point 4) and the temperature of the saturated liquid in 3′, defined by the manufacturer.

In order to determine Δh_{23}, which corresponds exactly to an enthalpy of desuperheating (segment 2–2′) of condensation (segment 2′–3′) and of subcooling (segment 3′–3), the enthalpy generated by the compression of the fluid in the process 1–2 must first be calculated.

The compression phase follows an isentropic curve in an ideal cycle (segment 1–2″). In the real case, there is a dissipation of energy due to the compressor efficiency, η_c, provided by the manufacturer and equal to 0.8. When the enthalpy and the pressure corresponding to point 1 are known, the

enthalpy at point 2″ can be calculated intersecting the isentropic at point 1 and the isobar at point 3. Consequently, point 2 can be obtained by inverting the following formula:

$$\eta_c = \frac{W_{id}}{W_r} = \frac{h_{2''} - h_1}{h_2 - h_1} \quad (13)$$

where:

W_{id} is the ideal work of compression process;

W_r is the real work of compression process;

$h_{2''}$ is the specific enthalpy of refrigerant obtained at the end of ideal compression process;

h_1 is the specific enthalpy of refrigerant obtained at the beginning of compression process;

h_2 is the specific enthalpy of refrigerant obtained at the end of real compression process.

Point 2 and then Δh_{23} can be calculated by knowing the enthalpy and the pressure corresponding to points 2 and 3, respectively.

Then, by once again applying the obtained relations through the thermodynamic properties, the real pressure values, p_h and p_c, and the actual refrigerant temperatures, T_h and T_c, are calculated. At this point the EER can be determined according to Equation (7).

2.3. Test Case

The described calculation model has been validated by comparing the calculated data with those monitored in an external test cell located at the ITC-CNR headquarters near Milan.

The test cell, with internal dimensions equal to 2.8 m × 5 m × 2.5 m (W × L × H) with a south-facing shorter side, is built with concrete loadbearing walls insulated with expanded polystyrene. Moreover, the south-facing wall is equipped with a glazed surface with an area of 3 m^2. The heating/cooling system is an inverter heat pump which may work in different configurations: cooling, dehumidification, ventilation and heating. The nominal cooling power is equal to 2.60 kW with an electrical power consumption of 0.65 kW. The internal airflow can be adjusted to three different values: 250, 300 and 500 m^3/h. The refrigerant fluid is R410A. Table 1 contains the manufacturer's information.

Table 1. Heat pump performance.

Efficiency Parameters	Nominal Condition	Value
Coefficient of Performance (COP)	20 °C DB 7 °C DB	4.26
Energy Efficiency Ratio (EER)	27 °C DB 35 °C DB	4.00

DB = Dry bulb.

The fluid flow rate is continuously regulated by the inverter that varies the compressor speed as a function of the thermal load. Several sensors to detect the indoor environmental parameters (air temperature, radiant temperature, air speed and relative humidity) are installed in the test cell, as shown in Figure 3.

The monitoring of the environmental and energy variables of the test cell was conducted from April to October 2014. The following analyses are referred to a typical summer week, for 13–19 August, allowing for a better comprehension of the results (Figure 4).

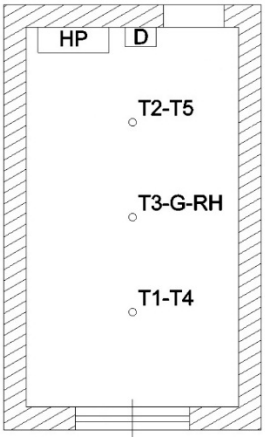

Figure 3. Plan of an outdoor test cell: HP (Heat Pump); D (Datalogger); T (Temperature sensors): T1 and T2 at 1.8 m in height, T4 and T5 at 0.5 m; G (Globe-thermometer); RH (Relative Humidity).

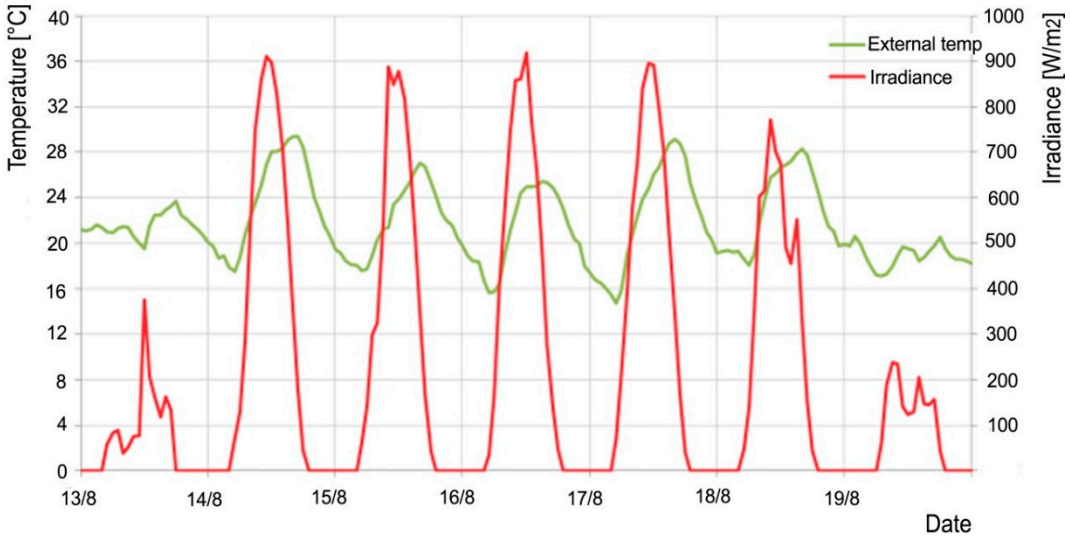

Figure 4. Weather data.

The thermal model of the envelope focuses on the idea of using the lumped solution's uttermost important features to build a 3R1C module (Figure 5) suitable for the representation of heat gains, losses and dynamic response of a single element of the building envelope. A whole system RC scheme is then assembled, connecting these modules according to the structure of the building envelope, through the internal air temperature node.

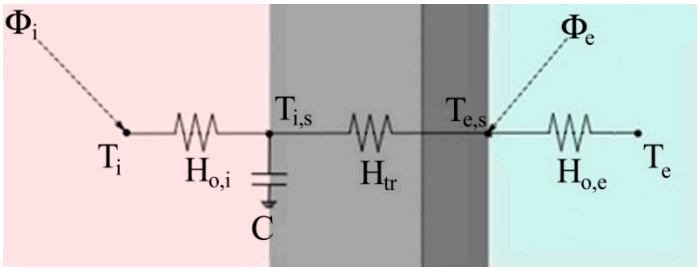

Figure 5. A 3 Resistance 1 Capacitance (3R1C) module.

The thermal mass of the system stores and releases heat according to instantaneous boundary conditions, both defined from the internal space ($T_{i,s}$ node) and external environment ($T_{e,s}$ node). The external air temperature node, T_e, is a boundary condition. This node is connected to the $T_{e,s}$ with an overall heat transfer coefficient $H_{o,e}$ (W/K), representing the convective and radiative surface heat exchange altogether. The internal temperature is determined by means of surface temperature values, $T_{i,s}$, as for the operative temperature, which describes internal conditions according to surfaces radiative and convective heat exchange, $H_{o,i}$ (EN ISO 13790). The obtained results are previously validated with the hourly measured data.

3. Results

3.1. Model Results

The first evaluation concerns the calculation of the EER. The calculation procedure is based on the second law efficiency, adapted to an hourly assessment. The method provides hourly values of EER, one for each time at which the heat pump is running. The results are shown in Figure 6.

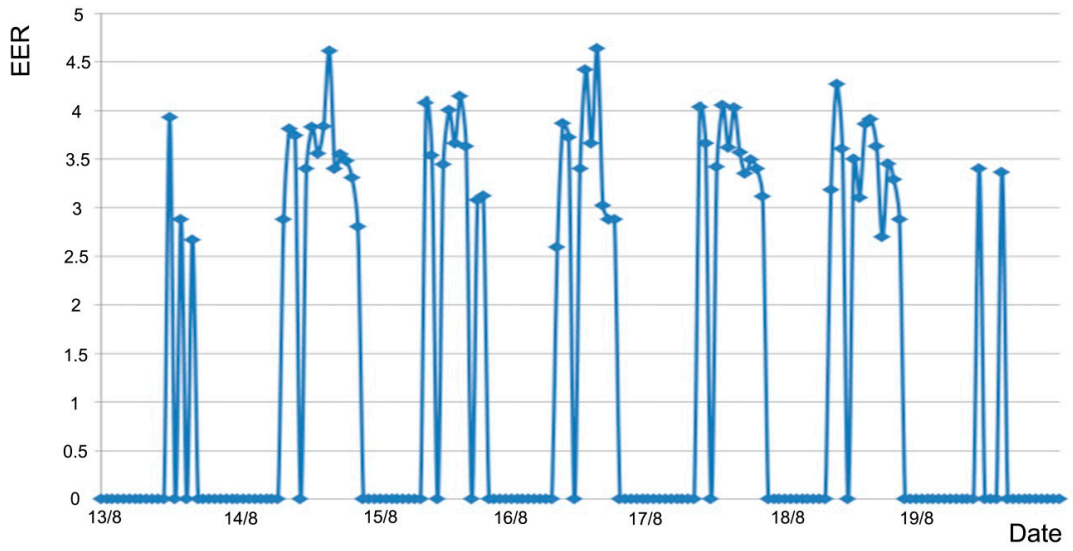

Figure 6. Calculated EER.

The EER values in the different running hours of the system are not constant but vary between 2.59 and 4.63. These results are in compliance with those expected, but 7% of the calculated values are lower than 3.2, which differ from what expected. The causes of this inconsistency may be found in the analysis of the refrigerant temperatures in the condenser and in the evaporator: the temperature of the cool reservoir, *i.e.*, in the evaporator, is much higher than the expected value. There is a correlation between these values and the cooling power; indeed, the EER outliers correspond to a cooling power lower than 350 W. The model shows an insufficiency in the modeling of the refrigerant flow rate modulation made by the inverter that causes an incorrect calculation of the refrigerant temperature in the evaporator.

The second step of the validation consists in the evaluation of the calculated energy consumption and in the relation with the outdoor temperature and the cooling power of the heat pump.

Figure 7 shows the trend of three cumulated energy consumptions over the experimental period: RC model, monitored and EnergyPlus v.8.4 cumulated consumptions. The test case was implemented in EnergyPlus using a direct expansion (DX) cooling coil and condensing unit, that includes an electric compressor and a condenser fan. The difference between the calculated (simplified model) and monitored consumption is equal to 2.1 kWh, and the final cumulated deviation is lower than 3%. The simplified model follows the real energy consumption well, always remaining below.

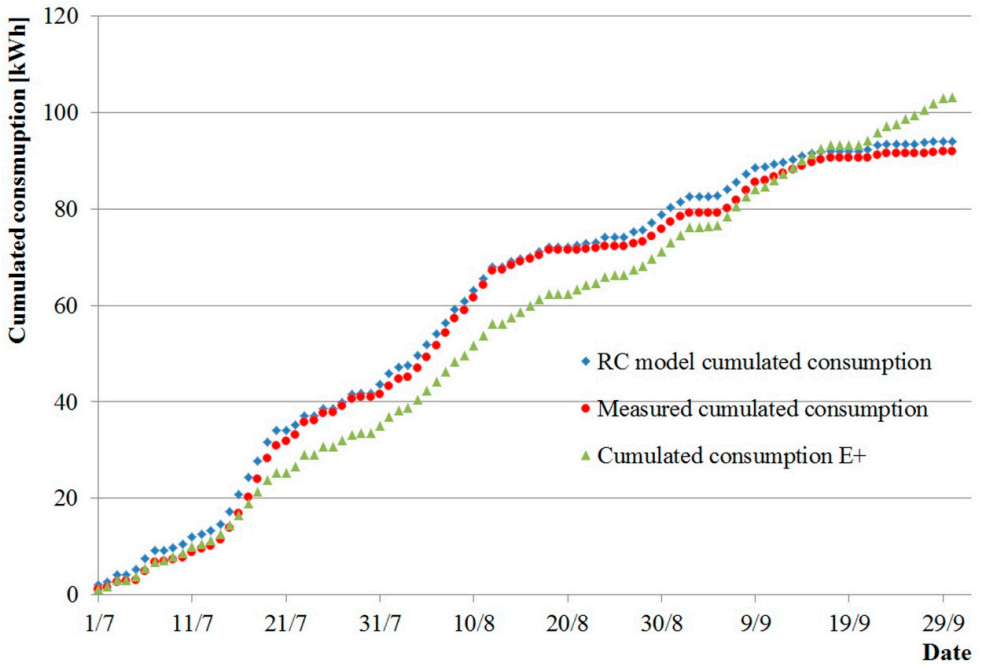

Figure 7. Cumulated consumptions.

The difference between the simplified model and EnergyPlus is equal to 9 kWh and lower than 9%. The EnergyPlus model is a black box that does allows to input physical numbers. In fact, the calculation of consumption is obtained through the determination of biquadratic and quadratic performance curves that parameterizes the variation of the energy input to cooling output ratio (EER), *i.e.*, as a function of the indoor wet-bulb temperature. The graph shows, however, that EnergyPlus overestimates the real consumption (11.9%).

Figure 8 shows the trend of the indoor temperature related to the calculated values with the simplified model (blue line), with the EnergyPlus v.8.4 model (orange line) and measured (red line). The green line represents the detected external temperature over the considered period. All the environmental parameters have hourly step representations. The trends of the calculated and measured data are almost equal except for the first hours of 13 August due the initialization of the simulation.

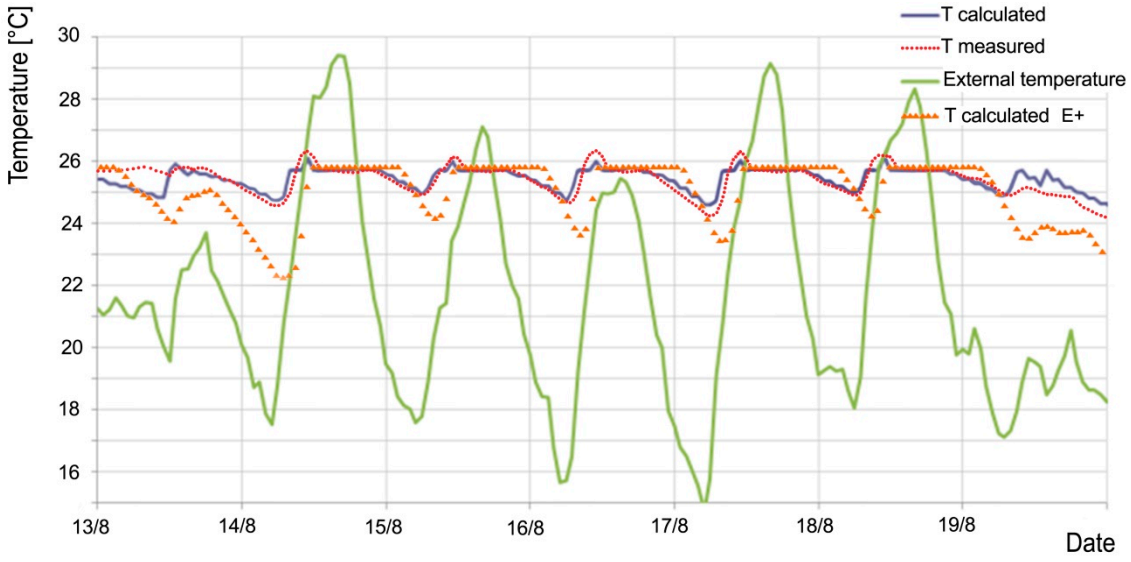

Figure 8. Indoor temperature comparison.

Different considerations can be carried out comparing the real data with the calculated data (simplified model). When the system is switched off, mainly in the nighttime, the indoor temperature is strongly dependent on the external temperature. The same correlation determines the trend of the energy consumption, directly proportional to the external temperature. A 3R1C (3 Resistance and 1 Capacitance) lumped model makes it possible to take into consideration the heat exchanges between the envelope components and the internal air mass.

During the running phase of the system, the model simulates the heat pump modulation of the refrigerant flow linked to the compressor speed variation.

Another aspect to be considered is the good behavior of the model toward the solar gain through the south-facing window. At noon, when the solar radiation comes into the cell and radiates a variable surface of the floor, peak temperature occurs indoors.

Introducing the EnergyPlus simulation it is possible to consider some differences. When the external temperature decreases, the internal temperature decreases very quickly. Furthermore, the solar gains behavior are not highlighted in the model. The last consideration refers to the operating hours of the heat pump that are shifted to a few hours.

Finally, in order to evaluate the sensitivity of the model to the environmental variables, the energy signature method has been applied, allowing to correlate the cooling energy consumption to the external temperature trend [36,37] between calculated and measured powers.

Figure 9 shows two rising fitting lines: the red one represents the measured average daily consumption and the blue one the calculated average daily consumption. The slopes of the line give information about the energy performance of the test cell. Both slopes and the intercepts are almost identical and equal to 15 W/K, showing a substantial parallelism of the lines. The results of the calculation model are very close to matching those monitored in the test cell.

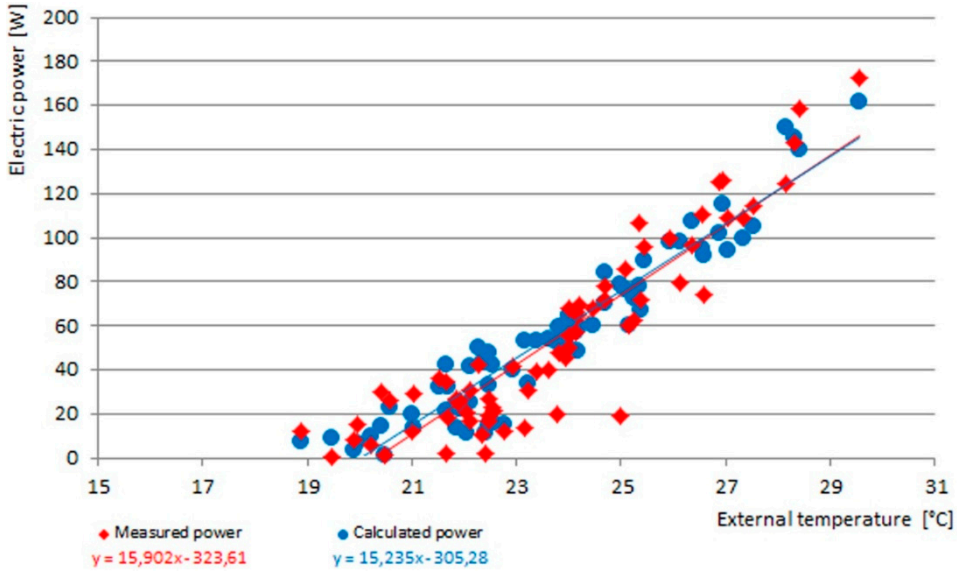

Figure 9. Comparison of the measured and calculated average daily powers through the energy signature method.

3.2. *Validation*

In order to reflect data consistency accurately (internal temperature and energy consumption) between the simulation and experimental data, the Bland-Altman test [38] is used in this paper.

In particular, when the graph points are within 95% confidence interval (Equation (14)), it can be affirmed that the two methods give consistent results.

$$I = \bar{x} \pm 1.96 \cdot s \quad (14)$$

where:

$\bar{x}$ is average differences,

s is standard deviations.

As regards the points that fall outside the confidence interval considered, it can be said that, in general, most of them are points scattered or spurious if they fall within the 99% confidence interval calculated as follows:

$$I = \bar{x} \pm 3 \cdot s \quad (15)$$

In any case, the points that fall outside the range of confidence are accepted as random or systematic errors.

Results reported in Table 2 show that the model give a better prediction of the internal temperature and the energy consumption. Results in terms of bias values referred to the considered time show that the model overestimates the plant power output for 0.8 W on average, while it underestimates the internal temperature for −0.22 K.

Table 2. Consistency verifications of model values and experimental results.

Indices	Average Differences between Calculated and Experimental Values—$\bar{x}$	Average Standard Deviations between Calculated and Experimental values—s	The 95% Confidence Interval	The 99% Confidence Interval
Indoor air temperature	−0.266 °C	0.616 °C	93.4	98.1
Energy consumption	0.989 Wh	52.907 Wh	92%	98.7%

Further characteristics can be deduced from plot visual analysis in terms of the internal temperature.

After careful analysis of the data, 93.4% of the points is placed within the confidence interval 95% (Figure 10). In order to define the nature of the points that fall outside the range considered, it has been expanded in the above range, as previously described. In this way, it is found that more than 98.1% of the points arise within a confidence interval of 99%, with a 4.7% difference that represents the number of spurious or scattered points.

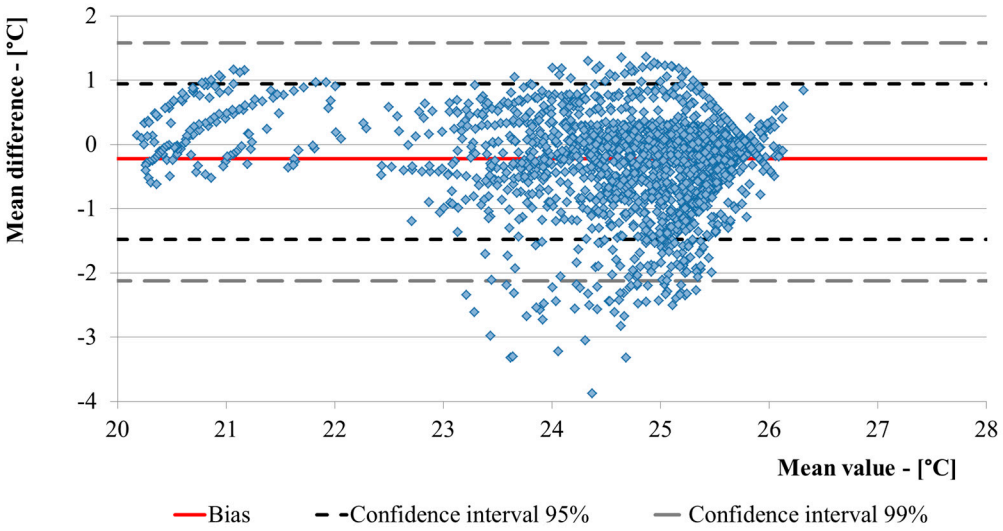

Figure 10. Bland-Altman plot: internal temperature.

It is possible to draw the same consideration in energy consumption (Figure 11). Starting from a confidence interval at 95%, 92% of the points fall inside. By extending the confidence interval at 99%, it is found that 98.7% fall within it.

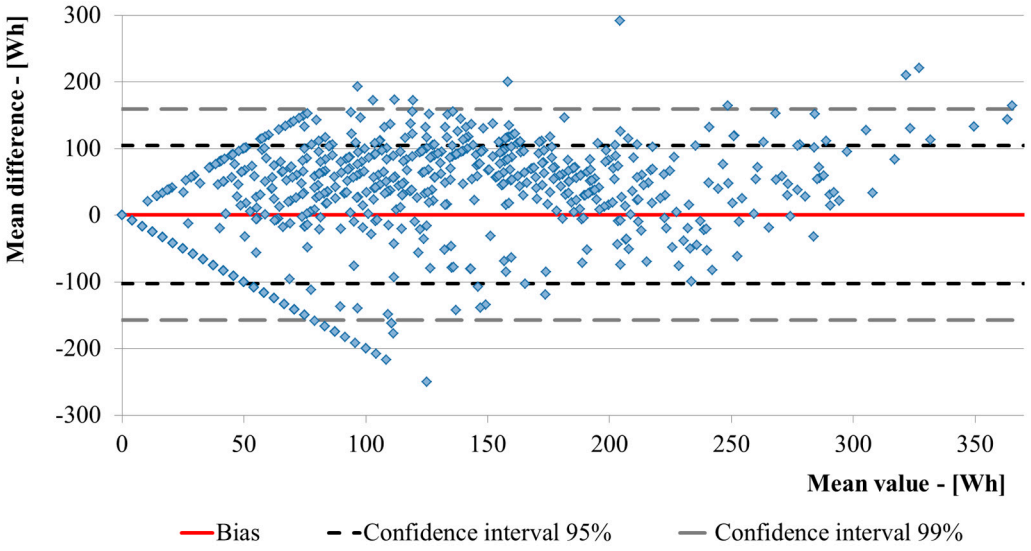

Figure 11. Bland-Altman plot: energy consumption.

Some values and outliers draw a line, which indicates that the ratio of the difference on the mean is constant for all these values. This particular correlation can be explained according to model results. The modelled heat pump supplies more inrush power than the real one.

4. Conclusions

This work aims at formulating a calculation model of the energy performance of a heat pump in cooling mode, which is able to provide results as close as possible to the real behavior of buildings in terms of indoor air temperature and energy consumption. Attention is focused on different configurations of the heat pump.

The updated model is based on the international standard EN 15316-4-2, providing for the application of the second law efficiency to a reversed Carnot cycle. The hourly consumption of the heat pump is based on the assessment of the COP or EER, calculated through the average hourly temperatures of the refrigerant fluid in the condenser and in the evaporator, determined through the reversed Carnot cycle.

An experimental campaign was conducted on an external test cell, aimed at validating the proposed calculation model; during the tests, the indoor temperatures and the energy consumption were monitored from April to October 2014. The simplified model was also compared with a dynamic simulation in order to investigate different approaches. On the one hand, the energy consumptions are close; on the other hand, the internal temperatures are very different. EnergyPlus is a black box that does not make it possible to understand the physical approaches used, and is studied in order to carry out an energy diagnosis of a building or parts of it. The calculated data with the suggested hourly calculation method demonstrate a high degree of accuracy in terms of energy consumption, indoor air temperature and energy signature with respect to the monitored data in order to correctly size a plant or maintain optimal indoor thermal comfort.

Most values are located within the confidence interval and good consistency was verified between values calculated by model and experimental results.

It should be noted that this model has been applied to a heat pump operating in the cooling mode. Possible future developments will provide for its generalization even in winter and for the assessment of the efficiency under different airflow rates that can be set by the user.

Author Contributions: The work presented in this paper is a collaborative development by all of the authors. In particular, I.M. has performed the preparation of the cell. F.S. has performed the analysis of the monitored data.

L.B. has performed the assessment of the energy consumption. L.D. has performed the hourly calculation method. M.M. has performed the dynamic simulation.

Conflicts of Interest: The authors declare no conflict of interest.

Nomenclature

Symbol	Term	Unit
COP	Coefficient of Performance	–
EER	Energy Efficiency Ratio	–
Q	Heat load	MJ
W	Energy supplied	MJ
T	Temperature	K
η	Efficiency	–
η_{II}	Second law efficiency	–
Δp	Pressure difference	Pa
Δh	Enthalpy difference	$kJ \cdot kg^{-1}$
DB	Dry Bulb	–
H	Heat transfer coefficient	W/K
C	Heat capacity	kJ/m^2
Φ	Heat flux	W/m^2

Subscripts

Symbol	Term
id	ideal
max	maximum
v	volumetric
iso	isentropic
h	hot source
c	cold source
h,1	hot source supplied by the manufacturer
h,2	hot source supplied by the manufacturer
c,1	cold source supplied by the manufacturer
c2	cold source supplied by the manufacturer
i	internal
e	external
s	surface
o	overall
tr	transmission

References

1. *Directive 2012/27/EU of the European Parliament and of the Council of 25 October 2012 on Energy Efficiency, Amending Directives 2009/125/EC and 2010/30/EU and Repealing Directives 2004/8/EC and 2006/32/EC*; The European Parliament and of the Council: Brussels, Belgium, 2012.
2. *Directive 2010/31/EU of the European Parliament and of the Council of 19 May 2010 on the Energy Performance of Buildings*; The European Parliament and of the Council: Brussels, Belgium, 2010.
3. Harish, V.S.K.V.; Kumar, A. A review on modeling and simulation of building energy systems. *Renew. Sustain. Energy Rev.* **2016**, *56*, 1272–1292. [CrossRef]
4. Ji, Y.; Xu, P. A bottom-up and procedural calibration method for building energy simulation models based on hourly electricity submetering data. *Energy* **2015**, *93*, 2337–2350. [CrossRef]

5. Terkaj, W.; Danza, L.; Devitofrancesco, A.; Gagliardo, S.; Ghellere, M.; Giannini, F.; Montic, M.; Pedriellia, G.; Sacco, M.; Salamone, F. A semantic framework for sustainable factories. *Procedia CIRP* **2014**, *17*, 547–552. [CrossRef]
6. Gagliardo, S.; Giannini, F.; Monti, M.; Pedrielli, G.; Terkaj, W.; Sacco, M.; Ghellere, M.; Salamone, F. An ontology-based framework for sustainable factories. *Comput. Aided Des. Appl.* **2015**, *12*, 198–207. [CrossRef]
7. Yan, D.; O'Brien, W.; Hong, T.; Feng, X.; Gunay, H.B.; Tahmasebi, F.; Mahdavi, A. Occupant behavior modeling for building performance simulation: Current state and future challenges. *Energy Build.* **2015**, *107*, 264–278. [CrossRef]
8. Salamone, F.; Belussi, L.; Danza, L.; Ghellere, M.; Meroni, I. An open source low-cost wireless control system for a forced circulation solar plant. *Sensors* **2015**, *15*, 27990–28004. [CrossRef] [PubMed]
9. Salamone, F.; Belussi, L.; Danza, L.; Ghellere, M.; Meroni, I. Design and development of nEMoS, an all-in-one, low-cost, web-connected and 3D-printed device for environmental analysis. *Sensors* **2015**, *15*, 13012–13027. [CrossRef] [PubMed]
10. Salamone, F.; Belussi, L.; Danza, L.; Ghellere, M.; Meroni, I. An open source "smart lamp" for the optimization of plant systems and thermal comfort of offices. *Sensors* **2016**, *16*. [CrossRef] [PubMed]
11. Zhu, M.; Pan, Y.; Huang, Z.; Xu, P. An alternative method to predict future weather data for building energy demand simulation under global climate change. *Energy Build.* **2016**, *113*, 74–86. [CrossRef]
12. *EN 15603:2008 Energy Performance of Buildings—Overall Energy Use and Definition of Energy Ratings*; CEN-European Committee for Standardization: Brussels, Belgium, 2008.
13. Van der Veken, J.; Saelens, D.; Verbeeck, G.; Hens, H. Comparison of steady-state and dynamic building energy simulation programs. In Proceedings of the International Buildings IX ASHRAE Conference on the Performance of Exterior Envelopes of Whole Buildings, Clearwater Beach, FL, USA, 5–10 December 2004.
14. Doyle, M.D. Investigation of Dynamic and Steady State Calculation Methodologies for Determination of Building Energy Performance in the Context of the EPBD. Master's Thesis, Dublin Institute of Technology, Dublin, Ireland, 2008.
15. Gasparella, A.; Pernigotto, G. Comparison of quasi-steady state and dynamic simulation approaches for the calculation of building energy needs: Thermal losses. In Proceedings of the International High Performance Buildings Conference, West Lafayette, IN, USA, 16–19 July 2012.
16. Belussi, L.; Danza, L.; Meroni, I.; Salamone, F.; Ragazzi, F.; Mililli, M. Energy performance of buildings: A study of the differences between assessment methods. In *Energy Consumption: Impacts of Human Activity, Current and Future Challenges, Environmental and Socio-Economic Effects*; Nova Science Publishers: New York, NY, USA.
17. Wauman, B.; Breesch, H.; Saelens, D. Evaluation of the accuracy of the implementation of dynamic effects in the quasi steady-state calculation method for school buildings. *Energy Build.* **2013**, *65*, 173–184. [CrossRef]
18. Fraisse, G.; Viardot, C.; Lafabrie, O.; Achard, G. Development of a simplified and accurate building model based on electrical analogy. *Energy Build.* **2002**, *34*, 1017–1031. [CrossRef]
19. Kampf, J.H.; Robinson, D. A simplified thermal model to support analysis of urban resource flows. *Energy Build.* **2007**, *39*, 445–453. [CrossRef]
20. Nielsen, T.R. Simple tool to evaluate energy demand and indoor environment in the early stages of building design. *Sol. Energy* **2005**, *78*, 73–83. [CrossRef]
21. Ramallo-González, A.P.; Eames, M.E.; Coley, D.A. Lumped parameter models for building thermal modelling: An analytic approach to simplifying complex multi-layered constructions. *Energy Build.* **2013**, *60*, 174–184. [CrossRef]
22. Park, H. Dynamic thermal modeling of electrical appliances for energy management of low energy buildings. In *Electric Power*; Universitè de Cergy Pontoise: Cergy Pontoise, France, 2013.
23. Amara, F.; Agbossou, K.; Cardenas, A.; Dubé, Y.; Kelouwani, S. Comparison and simulation of building thermal models for effective energy management. *Smart Grid Renew. Energy* **2015**, *6*, 95–112. [CrossRef]
24. Afram, A.; Janabi-Sharifi, F. Review of modeling methods for HVAC systems. *Appl. Therm. Eng.* **2014**, *67*, 507–519. [CrossRef]
25. Fong, J.; Edge, J.; Underwood, C.; Tindale, A.; Potter, S. Performance of a dynamic distributed element heat emitter model embedded into a third order lumped parameter building model. *Appl. Therm. Eng.* **2015**, *80*, 279–287. [CrossRef]

26. Cheung, H.; Braun, J.E. Component-based, gray-box modeling of ductless multi-split heat pump systems. *Int. J. Refrig.* **2014**, *38*, 30–45. [CrossRef]
27. Costanzo, G.T.; Sossan, F.; Marinelli, M.; Bacher, P.; Madsen, H. Grey-box modeling for system identification of household refrigerators: A step toward smart appliances. In Proceedings of the IEEE 2013 4th International Youth Conference on Energy, 6–8 June 2013; pp. 1–5.
28. Afram, A.; Janabi-Sharifi, F. Gray-box modeling and validation of residential HVAC system for control system design. *Appl. Energy* **2015**, *137*, 134–150. [CrossRef]
29. Reay, D.A.; Macmichael, D.B.A. *Heat Pumps*; Elsevier: Oxford, UK, 1988.
30. Crawley, D.B.; Pedersen, C.O.; Lawrie, L.K.; Winkelmann, F.C. EnergyPlus: Energy simulation program. *ASHRAE J.* **2000**, *42*, 49–56.
31. Danza, L.; Barozzi, B.; Belussi, L.; Meroni, I.; Salamone, F. Assessment of the performance of a ventilated window coupled with a heat recovery unit through the co-heating test. *Buildings* **2016**, *6*, 3. [CrossRef]
32. Nowak, T.; Jaganjacova, S.; Westring, P. *European Heat Pump Market and Statistics Report*; European Heat Pump Association: Brussels, Belgium, 2014.
33. Hannon, M.J. Raising the temperature of the UK heat pump market: Learning lessons from Finland. *Energy Policy* **2015**, *85*, 369–375. [CrossRef]
34. Cengel, Y.A. *Introduction to Thermodynamics and Heat Transfer*; McGraw-Hill Higher Education: Columbus, OH, USA, 2007.
35. *EN 15316-4-2:2008 Heating Systems in Buildings: Method for Calculation of System Energy Requirements and System Efficiencies; Part 4-2: Space Heating Generation Systems, Heat Pump Systems*; CEN-European Committee for Standardization: Brussels, Belgium, 2008.
36. Belussi, L.; Danza, L. Method for the prediction of malfunctions of buildings through real energy consumption analysis: Holistic and multidisciplinary approach of energy signature. *Energy Build.* **2012**, *55*, 715–720. [CrossRef]
37. Belussi, L.; Danza, L.; Meroni, I.; Salamone, F. Energy performance assessment with empirical methods: Application of energy signature. *Opto Electron. Rev.* **2015**, *23*, 85–89. [CrossRef]
38. Bland, J.M.; Altman, D.G. Statistical methods for assessing agreement between two methods of clinical measurement. *Int. J. Nurs. Stud.* **2010**, *47*, 931–936. [CrossRef]